IITRI

GPO PRICE $ _____

CSFTI PRICE(S) $ _____

Hard copy (HC) ___

Microfiche (MF) ___

ff 653 July 65

V6000-2
(Quarterly Report No. 2)

ANALYSIS OF CORONAL LINE PROFILES

N68-34067

(ACCESSION NUMBER) (THRU)

24 1

(PAGES) (CODE)

CR-96712 30

(NASA CR OR TMX OR AD NUMBER) (CATEGORY)

FACILITY FORM 602

SEP 1968

RECEIVED
NASA STI FACILITY
INPUT BRANCH

IIT Research Institute

V6000-2
(Quarterly Report No. 2)

ANALYSIS OF CORONAL LINE PROFILES

V6000-2
(Quarterly Report No. 2)

ANALYSIS OF CORONAL LINE PROFILES

Prepared by

Gordon Henderson

National Aeronautics and Space Administration
Washington, D. C.

Attention: Dr. Harold Glaser

IIT RESEARCH INSTITUTE

ABSTRACT

Coronal Fe XIV emission data obtained during the total solar eclipse of 12 November 1966 have been reduced to emission line profiles. The effects of non-linearities in wavelength scanning of the Fabry-Perot interferometer and of its instrumental broadening function were determined in the analysis of the relation between the observed profile and the true emission profile. The data are presented as emission line halfwidths and as temperature assuming pure thermal Doppler broadening for 49 positions out to 1.5 solar radii and for four positions from 1.6 to 2.0 solar radii.

FOREWORD

This is the second quarterly report for NASA Contract NASr-65(24) entitled, "Analysis of Coronal Line Profiles". This report constitutes the final report for Sub Task 1 of this contract which requires the reduction and analysis of the data obtained under NASA Contract Task Order NASr-65(12). The line profiles of the coronal Fe XIV emission observed during the total solar eclipse of 12 November 1966 have been reduced to provide line halfwidths versus solar position angle and radius. The analysis of the data includes discussion of source and instrumental effects influencing the line profile and the interpretation of halfwidth in terms of temperature.

Respectfully submitted,

IIT RESEARCH INSTITUTE

Robert W. Deuel

Robert W. Deuel
Associate Physicist
Plasma Physics Research

APPROVED BY:

W O Davies

William O. Davies
Assistant Director
Physics Division

ANALYSIS OF CORONAL LINE PROFILES

I. INTRODUCTION

The existence of temperatures of the order of a million degrees in the solar corona has been accepted generally since about 1945. Present research into coronal temperature is directed towards more accurate measurements with higher spatial resolution and a more rigorous examination of the variance due to the different methods of measuring the coronal temperature. These studies are essential in order to understand the physics of the corona.

The method of temperature measurement of a plasma by high resolution spectroscopy of emission line widths has become a widely accepted technique in both physics and astronomy since the end of the last century. Buisson, Fabry and Bourget (1914) were the first workers to apply the Fabry-Perot interferometer for this purpose when they measured the interference fringes formed by emissions in the Orion Nebula. During the eclipse of 1954 Jarrett and von Kluber (1955) first obtained fringes from the coronal λ 5303 A (Fe XIV) emission using a Fabry-Perot interferometer. They repeated their observations during the eclipse of 1958 when they also obtained interference fringes from the λ 6374 A (Fe X) emission (Jarrett and von Kluber 1958).

The observations described in this report are an extension of their technique using photoelectric detection and spectral scanning

by magnetostrictive displacement of the interferometer plates. The observations were made during the eclipse of 12 November 1966 from the NASA aircraft "Galileo" which provided a high altitude observing platform.

This report describes the analysis of the data which consists of the following tasks:

a) determine the position of the field of view with respect to the eclipsed sun for each line profile.

b) correct the observed line profile for instrumental broadening and electrical/mechanical non-linearities.

c) relate the line width to temperature assuming pure Doppler broadening by thermal processes.

II. DESCRIPTION OF THE OBSERVATION

A. Equipment

The general layout of the optical system is shown in Figure 1. Light from the corona is directed to the objective via the variable wedge and folding mirror. The objective focuses the field onto the aperture whose size governs the angle of acceptance of the telescope. In operation, the system is initially aligned on the sun's center with the variable wedge aligned to have zero effect on the incoming light; the two composite wedges can have any orientation relative to each other, the resultant effect upon a light beam being similar to that of a single wedge at a specific orientation. Hence for a fixed relative orientation of the component wedges, the field of view is deflected by a specific amount, and rotation of the complete assembly about the optic axis provides a circular sweep of the field. After the initial alignment, the gyro-stabilized heliostat is locked-in and a relative rotation of the wedge assembly to the first position brings the region of the corona at 1.1 $R_\odot$, onto the aperture where $R_\odot$ is one solar radius.

B. Pointing and Field of View

The field of view defined by the entrance aperture was 1.45 minutes of arc or 0.09 $R_\odot$ at the time of eclipse. The

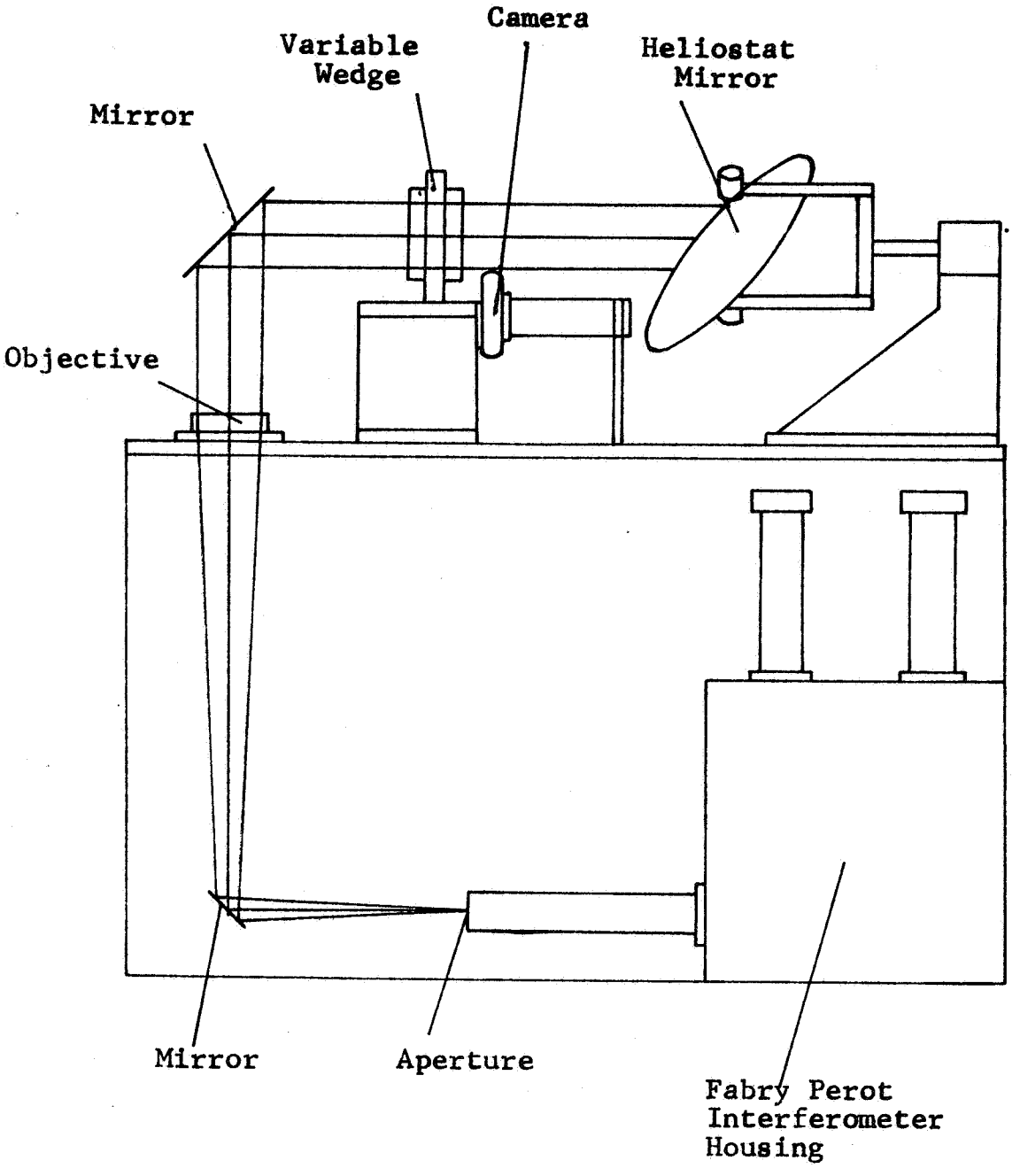

Fig. 1 Showing the General Layout of the Optical System for the Aircraft Installation to Investigate Coronal Emission Profiles.

technique employed to scan the corona was such that a continuous 360° rotation in position angle at a constant radius was performed in 13 seconds. The radius then changed automatically and the rotation proceeded again. The spectral scanning rate was such that the dwell time in a typical emission feature was about 0.1 second. Hence the smearing in position angle due to the motion of the positional scanner was 2.8 degrees.

During the eclipse, the drive system of the wedge assembly provides a rotation of the field at the selected radial distance from the sun's center. After each rotation, an automatic change in radius is made and the rotation is repeated. This operation takes place continuously during the eclipse, and a continuous recording of the position of the field of view is made.

Figure 2 shows the optical arrangement after the light has passed through the aperture. Coronal light transmitted by the aperture is collimated at the entrance to the interferometer housing. Two scanning Fabry-Perot interferometers are installed to provide a redundant system; the design is such that the back-up Fabry-Perot is used to provide scans of the λ6374 A (Fe X) emission line while the main interferometer is scanning the λ 5303 A (Fe XIV) emission. Both emissions are obtained from the same field of view defined by the field aperture. Should the λ 5303 A unit or its associated circuitry fail during the observations, the system can be changed to the back-up instrument in about 10 seconds.

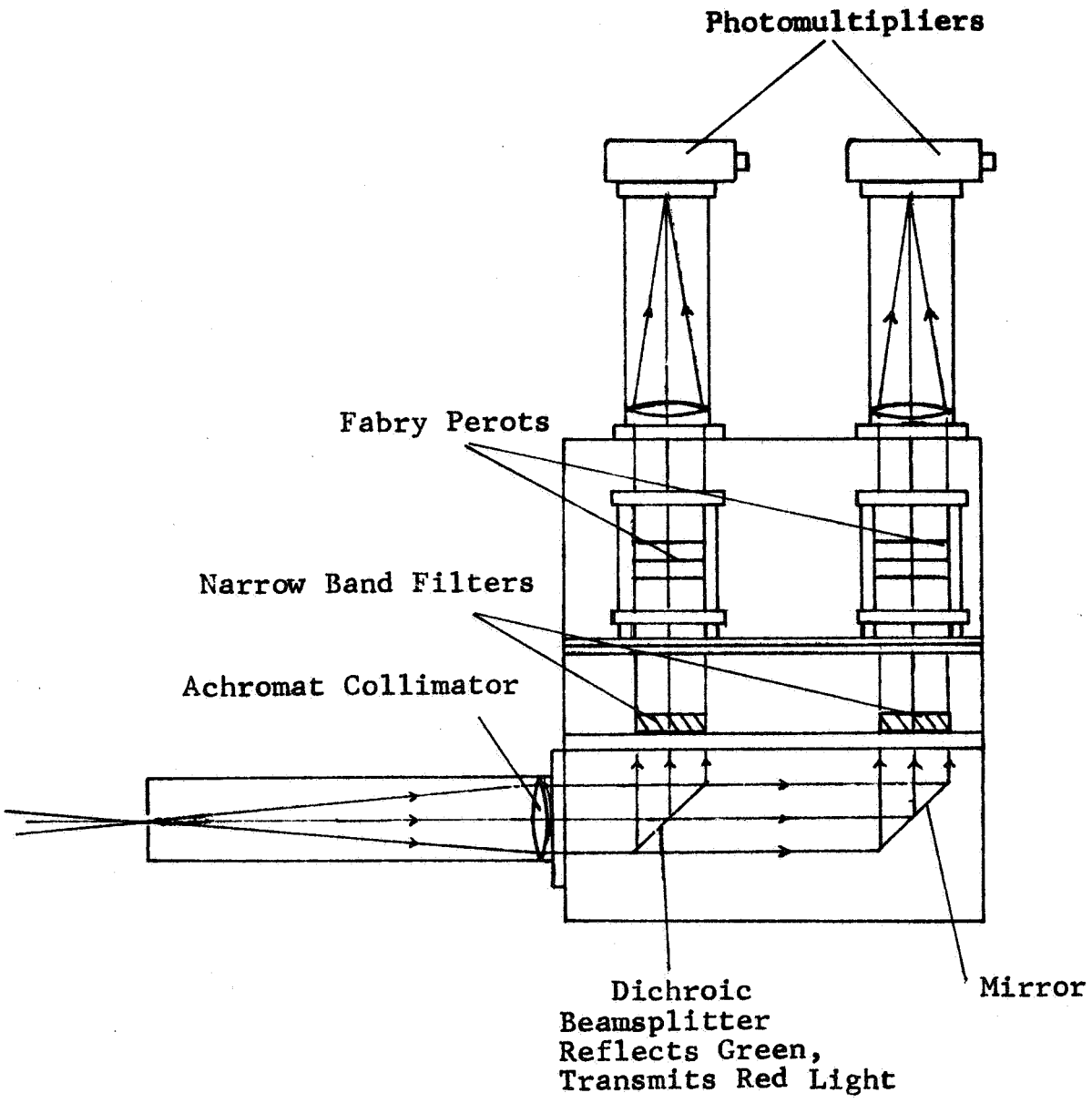

Fig. 2 Showing Layout of Two Fabry Perot Interferometers to Record λ5303A and λ6374A Emission Profiles

After passing through the entrance aperture the coronal light was collimated before falling on a dichroic beamsplitter set at 45° to the incident light. By the action of the beamsplitter, the red and green regions of the spectrum were separated and each passed through a 5 A half width multilayer dielectric forefilter centered respectively on λ 6374 A and λ 5303 A. After passing through the forefilters, each light beam passed through an interferometer which scanned through a spectral region of about 3.5 A with a spectral resolution of about 0.14 A. The light transmitted by each interferometer was focused onto photomultiplier tubes whose outputs were amplified and recorded on a high speed strip chart recorder. Continuous visual monitoring of the outputs of both interferometers during operation was provided by an oscilloscope and, hence, a failure of either interferometer system would be immediately apparent.

The short term stability of the pointing system was designed to give an accuracy of $\pm$ 10 seconds of arc. During two nighttime practive flights, star images were observed on the aperture screen under magnification and no discernable rapid movement took place. If we regard an oscillation of 0.5 mm amplitude as discernable then the pointing was better than 1.0 minute of arc over periods of less than a few seconds.

III. ANALYSIS OF THE DATA

A. Position of the Field of View

The analog data record contained information regarding the pointing of the instrument with respect to solar position angle and radius.

Corrections were required for the positional information as follows:

1) A correction was made to account for multiple oblique reflections in the optical system; this was measured before the eclipse flight using a vertical line on the viewing post. An important check was obtained during the eclipse from the position of the planet Venus relative to the sun as measured on a photograph taken during totality. The camera looked into the gyro stabilized heliostat and was rigidly attached to the instrument frame.
2) A correction was made for the slow drift of the gyro stabilized platform; this correction was obtained by measuring the total drift of the solar image over the period of totality on the aperture plate of the telescope. Assuming that the rate was constant, a correction for each radius and position angle was obtained by

interpolation. The maximum amount of this correction occurred for the last readings since the sun's image was initially centered on the aperture. The amount of the maximum correction was 0.06 $R_\odot$ in radius and 3° in position angle.

3) A correction was made for changes in aircraft trim; the aircraft flew nose up (2°) during the eclipse flight and this required a correction of a similar amount to obtain the local vertical.

B. Derivation of Emission Profile

The data record for the λ 5303 A emission shown in Figure 3 contains a regular noise component with a frequency of several hundred cycles per second. The first task in obtaining the true emission profile was to smooth these data by hand. A correction was then made for a slight difference in the scanning rate between decreasing and increasing current. The next step in the analysis of the data was to compensate for non-linear effects in the spectral scan. Such effects may be due to two possible causes, non-linearity in the scanning current or non-linearity of the magneto-strictive effect as saturation occurs. The form of the scanning current is shown in Figure 3 to be linear except for the last 15 percent near maximum current. Since the emission profiles fell on the linear portion of the scan

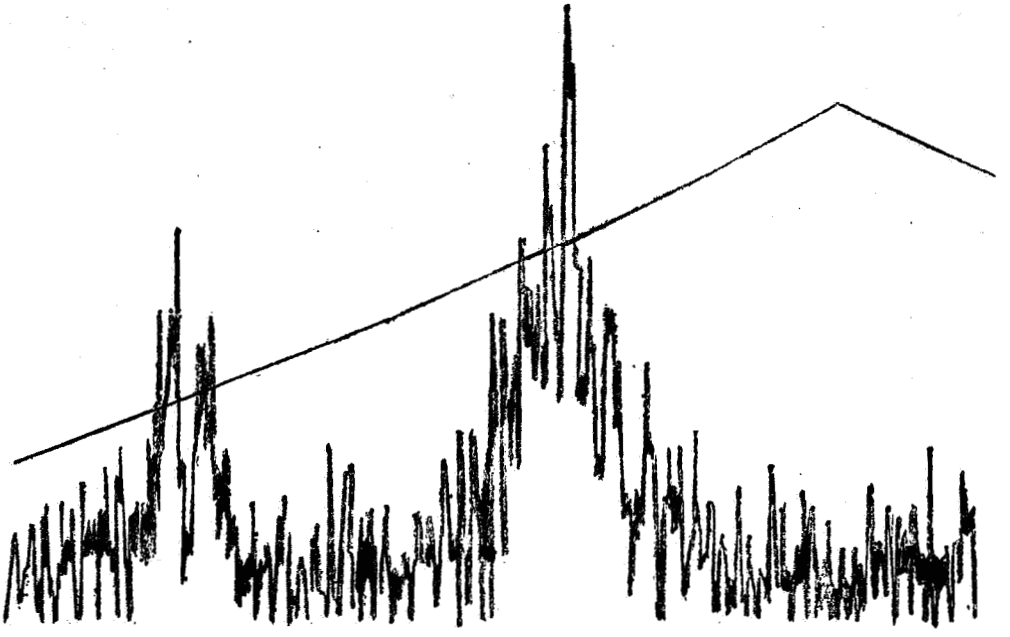

Fig. 3 Data Record for 5303 A Coronal Emission

we can neglect the effect of non-linearity in the scanning current. To determine non-linearity of the magneto-strictive effect, a series of measurements of the 5461 A emission from a low pressure mercury lamp were made before and after eclipse totality. The variation in the halfwidth of the mercury line profile appearing in different orders at different currents provided a calibration of the instrumental broadening function versus current. A further measure of the effect of non-linearity in the magneto-strictive effect of the interferometer was obtained from initial spectral scans of the coronal emission at a fixed position. Four first order profiles were obtained at a lower value of scanning current and four second order profiles at a higher value of current. The widths of the observed profiles were compared for the different values of current to provide the correction. The difference in profile width between orders was then ascribed to non-linearity in the magnetostrictive effect.

The instrumental width at half intensity (or half width) was obtained from the traces of the λ5461 A Hg emission made before and after the eclipse. The measured half width was 0.135 A; since the half width of the emission from the low pressure mercury lamp is significantly less than this, it was assumed that all of the line broadening was due to the instrumental effect. Hence, the instrumental half width is 0.135 A. Correction for the instrumental effect was then made by using a sum of squares technique:

$$\Delta\lambda^2_{obs} = \Delta\lambda^2_{line} + \Delta\lambda^2_{inst} \qquad (1)$$

C. Relation of Temperature to the Emission Profile

The half width of a thermally Doppler broadened line is related to temperature by the following equation:

$$T = \frac{\Delta\lambda^2 M}{(7.16 \times 10^{-7} \lambda)^2} \qquad (2)$$

where T is the temperature in degrees Kelvin; $\Delta\lambda$ is the half width of the corrected profile in A; M is the mean atomic weight of the emitting ion, and λ is the wavelength in A. Using these values for the parameters, equation (2) becomes:

$$T = 3.85 \times 10^6 \quad (\Delta\lambda^2_{obs} - \Delta\lambda^2_{inst}) \quad . \qquad (3)$$

IV. INTERPRETATION OF LINE PROFILES TO DETERMINE TEMPERATURE

In considering the various processes by which emission lines may be broadened in the corona all processes except thermal and macroscopic line of sight motions are generally neglected. Many observations have been made in an attempt to establish the relative importance of thermal and macroscopic motions. Billings (1966) gives a survey of the contributions to this study and concludes that net macroscopic line-of-sight motions make little contribution to the observed line widths. The principle support for this conclusion is given by the fact that actual Doppler shifts of the emission peak were rare and when present were very small.

The detected coronal emission during a single spectral scan is made up of contributions from all volume elements within the field of view. Billings (1964 and 1966) discusses several distortion effects which can broaden coronal emission without producing displacement or asymmetry. These include circulatory and oscillatory motions in which the field of view includes whole numbers of such systems and also sysmmetric inflow or outflow of matter from each feature. All of these motion types result in similar distortions of a thermal Gaussian profile.

There is also the case where the line-of-sight includes several features at different temperatures which produce a superposition of different thermal halfwidths. The net result of this type of summation is a profile which is also distorted

from a Gaussian profile but in a manner nearly opposite to that produced by motion distortion. Thus, the presence of both types in varying degrees results in a cancellation of effects although the resultant indicates the dominant mode.

It appears then that line profile measurements cannot be unambiguously related to temperature by pure Doppler broadening calculations but may be so interpreted bearing in mind these possible sources of error. The data from this experiment will be presented in tabular form giving both line halfwidths and Doppler temperatures as a function of solar position angle and radius and as temperature on an overlay plot of a photograph of the corona taken during this eclipse. The photograph was provided through the courtesy of Dr. Gordon Newkirk, High Altitude Observatory, Boulder, Colorado.

V. RESULTS

Spectral scanning of the coronal λ 5303 A emission was conducted in two successive groups. The first group is presented in Table I and formed the major portion of the data (i.e. 49 separate emission profiles). These were obtained at a scanning rate of one profile every 0.25 second, the dwell time in the emission being about 0.1 second. When the signal to noise ratio became small, the second group, shown in Table II, was obtained at a much slower scan rate; the scanning was done by hand at approximately one scan per 2-3 seconds. The corona positional scanner was switched off during these slower scans and the position angle was set near 265°. In all, four sets of four scans each were obtained in the second group, giving four mean temperature values as indicated in Table II.

The tables present the line widths and derived temperatures for each position in the corona where data were obtained versus the position angle (θ referred to the projected position of the north pole on the solar disk) and the corrected radial distance relative to the sun's center in units of the solar radius. Figure 4 shows the temperature map superimposed on the photograph of the corona. Estimated accuracy in line width measurements is $\pm$ 25% which gives an accuracy of $\pm$ 50% in the derived temperatures.

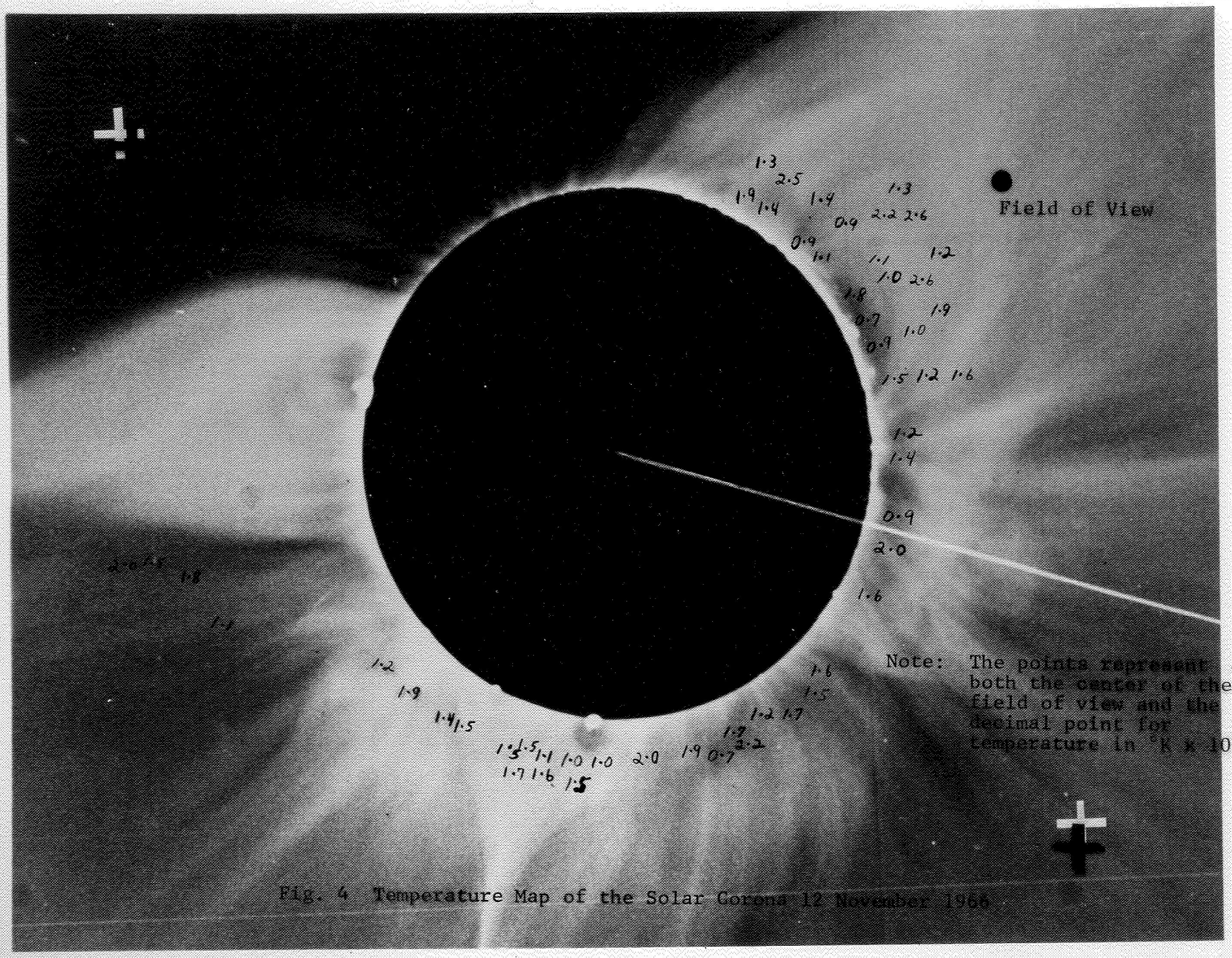

Fig. 4 Temperature Map of the Solar Corona 12 November 1966

Photograph: Courtesy of High Altitude Observatory, Boulder, Colorado

TABLE I

Fe XIV Emission Line Halfwidths and Temperatures

Position Angle	Radius	Halfwidth	Temperature ($°K \times 10^{-6}$)
319	1.15	.566	1.1
316	1.15	.616	1.5
313	1.16	.613	1.5
303	1.18	.624	1.5
298	1.19	.611	1.4
291	1.20	.701	1.9
284	1.21	.553	1.2
131	1.19	.694	1.9
126	1.19	.611	1.4
117	1.17	.494	0.9
112	1.16	.537	1.1
102	1.15	.689	1.8
097	1.14	.428	0.7
091	1.13	.488	0.9
084	1.13	.618	1.5
073	1.11	.506	1.0
068	1.10	.595	1.4
056	1.10	.492	0.9
049	1.10	.722	2.0
038	1.09	.653	1.6
020	1.10	.643	1.6
015	1.10	----	---
005	1.10	.561	1.2
358	1.11	.537	1.1
349	1.12	.701	1.9
340	1.13	.727	2.0
331	1.14	.518	1.0
325	1.15	.518	1.0

TABLE I (continued)

Position Angle	Radius	Halfwidth	Temperature ($°K \times 10^{-6}$)
315	1.24	.666	1.7
308	1.25	----	---
017	1.15	.628	1.5
010	1.16	.672	1.7
000	1.17	.752	2.2
354	1.18	.440	0.7
326	1.22	.631	1.5
320	1.23	.651	1.6
130	1.36	.578	1.3
125	1.34	.807	2.5
118	1.34	.611	1.4
113	1.32	.480	0.9
104	1.31	.522	1.1
100	1.30	.509	1.0
090	1.28	.514	1.0
083	1.26	.558	1.2
108	1.45	.758	2.2
097	1.43	.826	2.6
092	1.41	.699	1.9
081	1.40	.647	1.6
070	1.39	----	---
110	1.56	.580	1.3
106	1.55	.828	2.6
101	1.54	----	---
099	1.53	.554	1.2

TABLE II

Fe XIV Emission Line Halfwidths and Temperatures

Position Angle	Radius	Temperature ($°K \times 10^{-6}$)	Mean Temperature	Halfwidth
260	1.70	1.3		.580
260	1.70	1.4		.594
260	1.70	1.0		.500
260	1.70	0.7	1.1	.425
258	1.78	1.9		.709
258	1.78	1.7		.660
258	1.78	1.8		.675
258	1.78	2.1		.738
258	1.78	1.5	1.8	.620
256	1.91	2.0		.719
256	1.91	1.5		.616
256	1.91	0.9		.483
256	1.91	---	1.5	----
255	2.00	1.7		.655
255	2.00	2.2		.762
255	2.00	2.5		.811
255	2.00	1.4	2.0	.602

REFERENCES

Billings, D. E. (1959) Ap. J., 130, p. 961.

Billings, D. E. (1964) Ap. J. 139, p. 710.

Billings, D. E. (1966) "A Guide to the Solar Corona", Academic Press, p. 246.

Buisson, H. Ch. Fabry and H. Bourget (1914) Ap. J., 40, p. 241.

Jarrett, A. H. and H. von Kluber, (1955) M.N., R.A.S., 115, 4, p. 343.

Jarrett, A. H. and H. von Kluber (1961) M.N., R.A.S., 122, 3, p. 223.